RAB10 involving in glucose uptake by regulating GLUT1 predicts poor prognosis in pancreatic cancer

Lijie Cai
Dalian Medical University
Jinrui Han
Dalian Medical University
Junqing Wu
Yangzhou University
Xinyu Ge
Dalian Medical University
Peng Liu
Yangzhou University
Heng Duan
Dalian Medical University
Tongtai Liu
Northern Jiangsu People's Hospital
Jie Yao (dryaojie@yzu.edu.cn)
Northern Jiangsu People's Hospital

Research Article

Keywords: RAB10, PAAD, Glucose uptake, Metabolic reprogramming, GLUT1

Posted Date: May 24th, 2022

DOI: https://doi.org/10.21203/rs.3.rs-1671317/v1

Abstract

Introduction: Pancreatic adenocarcinoma (PAAD) is a lethal cancer, and metabolic reprogramming in PAAD is a clinical concern. The RAS oncogene family member RAB10 is highly expressed in many tumor tissues, but its role in PAAD remains unclear. Here, we explore correlations between RAB10 expression and PAAD prognosis. This study investigated whether RAB10 regulates glucose uptake in PAAD cells through modulating the expression and location of the glucose transporter1 (GLUT1).

Methods: Immunohistochemical staining was used to detect the expression of RAB10 in pancreaticoduodenectomy specimens. The function of PAAD cells expressing different levels of RAB10 was assessed by CCK-8 proliferation, wound healing, and transwell migration assays. Glucose uptake assays and lactate production assays were used to explore the effects of RAB10 on PAAD cell metabolism. In addition, we used qRT-PCR, western blot, and immunofluorescence to analyze interactions between RAB10 and GLUT members.

Results: RAB10 was highly expressed in PAAD tissues and cell lines, and was significantly correlated with T classification and pathological differentiation. High RAB10 expression was found to be an independent prognostic factor of poor disease outcomes in PAAD. RAB10 knockdown inhibited proliferation, invasion, and metastasis of PAAD cells, and downregulated glucose uptake and lactate production. Down-regulation of RAB10 inhibited GLUT1 translocating to the cell membrane and downregulated GLUT1 expression, which in turn decreased glucose uptake in tumor cells.

Conclusion: These results demonstrate that overexpression of RAB10 is associated with worse PAAD survival outcomes. Downregulation of RAB10 may decrease glucose uptake in tumor cells by inhibiting GLUT1 membrane localization and downregulating GLUT1 expression.

1. Introduction

Pancreatic adenocarcinoma (PAAD) is the fourth leading cause of cancer death, with a five year survival rate of 9% through 2020 [1]. PAAD accounts for about 90% of pancreatic cancer and is the primary cause of pancreatic cancer mortality [2]. PAAD cells have extensively reprogrammed metabolism, whereby they maintain the constant energy demand to support tumorigenesis and aggressiveness [3]. One of the most common and important metabolic changes in PAAD is a shift to aerobic glycolysis, known as the "Warburg effect". This effect causes cancer cells to preferentially consume more glucose and produce more lactic acid, which facilitates acidification of the tumor microenvironment to favor tumor invasion and metastasis [4, 5].

RAB10 is a member of the small molecule GTPase family and is mainly involved in vesicle transport of proteins [6]. In recent years, RAB10 has been found to regulated the transfer of glucose transporter solute carrier family 2 member 4 (facilitated glucose transporter 4, GLUT4) to the cell membrane, thereby improving the glucose uptake capacity of muscle cells and adipocytes [7, 8]. RAB10 is activated by Rab

GTPase activating protein (GAP) TBC1D4, and is the main Rab GTPase involved in the transfer of GLUT4 to the cell membrane in adipocytes [9, 10]. In addition, RAB10 is highly expressed in gastric cancer, breast cancer, glioma, and other malignant tumors, and high expression of RAB10 is associated with poor prognosis [11–16]. The role of RAB10 in PAAD has not yet been explored, and the relationship between RAB10 and the pathogenesis or progression of PAAD is uncertain. The purpose of this study was to explore the correlation between the RAB10 expression and prognosis of PAAD, and to explore possible molecular mechanisms of action of RAB10 in PAAD.

2. Materials And Methods

2.1 Patients and specimens

Tissue samples for this study were obtained from resected specimens of patients who underwent pancreaticoduodenectomy from January 2016 to December 2019 in Northern Jiangsu People's Hospital. We selected specimens with postoperative pathological findings of pancreatic ductal adenocarcinoma as the tumor group; none of these specimens underwent preoperative radiotherapy or chemotherapy. We selected specimens of non-pancreatic tumors (such as duodenal papilloma or extrahepatic bile duct malignancies), and removed individuals with pancreatitis and pancreatic tumor metastasis as the normal group. Ultimately, we obtained 86 PAAD tissue samples and 55 normal pancreatic tissue samples. Follow-up and clinicopathological data were collected from patients in all groups. The samples used in the study were obtained from the Department of Biobank, Subei People's Hospital of Jiangsu province. Standards from the American Joint Committee on Cancer (AJCC) [17] were used to guide tumor staging and classification. The latest follow-up time point for this study was January 1, 2022.

2.2 Cell lines and cell culture

The Shanghai Institute of Nutrition and Health, China provided the following human cell lines: HPDE, PANC-1, SW1990, AsPC-1, CFPAC-1, and HPAF-II. HPDE cells are normal pancreatic ductal epithelial cells. PANC-1 and HPAF-II are human PAAD cell lines. SW1990 was derived from human spleen metastatic PAAD cells. AsPC-1 was derived from human ascites metastatic PAAD cells. CFPAC-1 cells are human liver metastatic PAAD cells. Cells were cultured in Dulbecco's modified Eagle's medium with 100 U/ml penicillin, 100 μg/ml streptomycin, and 10% fetal bovine serum. All cells were grown in a humidified incubator with 5 % CO_2 at 37°C

2.3 Immunohistochemistry (IHC)

The RAB10 antibody was used at a concentration of 1:100, and was purchased from Beijing Bioss Biotechnology Co., Ltd. (Beijing, China). Briefly, cells were incubated with goat anti-rabbit antibody conjugated with horseradish peroxidase (HRP) at room temperature for 50 min. Cells were then stained using a 3,3'-diaminobenzidine reagent kit, and re-stained using hematoxylin. RAB10 staining evaluation included staining intensity (score 0: no staining; 1: weak coloring; 2: moderate staining; 3: strong staining) and the percentage of positively stained cells (score 0: <10%; 1: 10-50%; 2: 51-80%; 3: >80%). We

multiplied the two scores together to produce a comprehensive expression score of 0-9, where 0 is negative, 1-4 is weakly positive, and > 4 is strongly positive.

2.4 RNA extraction and qRT-PCR

TRIzol reagent (Invitrogen, China, Shanghai) was used to extract total RNA from cells and tissues. cDNA was reverse transcribed from the mRNA using a PrimeScript RT Reagent Kit (Takara, Shiga, Japan) and quantitative real-time PCR (qPCR) kits were purchased from Vazyme (Nanjing, China). The qRT-PCR assay was performed according to the MIQE guidelines [18]. The primers used are listed in Supplementary Table 1.

2.5 Transfection of short interfering RNA (siRNA)

The siRNA targeting RAB10 (si-RAB10) and negative controls were obtained from GenePharma (Shanghai, China). Briefly, siRNAs and controls were transfected into PANC-1 and CFPAC-1 cells at 70–80% confluence in 6-well plates, using Lipofectamine 2000 (GenePharma). Quantitative real-time reverse transcription PCR (qRT-PCR) was used to determine the transfection efficiency. The sequences of gene-specific siRNAs are shown in Supplementary Table 2.

2.6 Western blot analysis

Total proteins were extracted from cells using radioimmunoprecipitation assay (RIPA) buffer (Beyotime biotechnology, Shanghai, China) with protease inhibitors. A bicinchoninic acid (BCA) Protein Assay Kit (Beyotime biotechnology, Shanghai, China) was used to determine the total protein content. Proteins were separated using 10% sodium dodecyl sulfate–polyacrylamide gel electrophoresis (SDS-PAGE), and were then transferred electrophoretically onto a polyvinylidene fluoride membrane. Membranes were blocked for 1 h in 5% skim milk powder in Tris-buffered saline + Tween 20 (TBST). Thereafter, primary antibodies were added at an appropriate dilution and incubated at 4ºC overnight. The primary antibodies comprised anti-RAB10 (Proteintech, 11808-1-AP), anti-GLUT1 (Proteintech, 21829-1-AP), and anti-GLUT3 (Proteintech, 20403-1-AP). The membrane was washed using TBST, and then incubated with HRP conjugated goat anti-rabbit antibody for 1 h. Protein bands were detected using ECL chemiluminescence.

2.7 Cell viability assay

A Cell Counting Kit 8 (CCK-8) kit assay (Beyotime Biotechnology) was used to evaluate cell viability. Following the supplier's protocol, cell suspension was seeded at 100 µL/well in 96 well plates and incubated for 12, 24, and 48 h. CCK-8 solution (10 µL) was added to each well of the plate, and incubated for 1–4 h. A microplate reader was used to measure the absorbance at 450 nm.

2.8 Wound healing scratch test

Cells in the logarithmic growth phase were digested and centrifuged, and plated at ~5×10^6 cells/well into a 6-well plate. After the cells had adhered, thee scratches were made in well and cells were cultured for 24

hours. During this time, images were recorded using a 100× microscope. The culture was continued for 24 hours and then then fresh medium was replaced, and images were recorded.

2.9 Transwell migration assay

Cells were cultured in the logarithmic growth phase, digested, washed with PBS and serum-free medium successively, then suspended with serum-free medium, counted, and adjusted to 2×10^5/mL. Next, 600-800 μL culture medium containing 10% serum was added to the bottom of a 24-well plate, and then 100-150 μL cell suspension was added to the transwell insert and cultured in an incubator for 24 h. Following 24 h, the lower surface was immersed in 4% paraformaldehyde solution to fix for 30-60 min, then was stained with crystal violet or trypan blue. After staining, the transwell inserts were imaged, and the number of cells on the lower surface of the PET film was calculated by taking 5 representative fields in the middle and around, and taking the mean value per field.

2.10 Detection of glucose consumption and lactate production assay

Transfected cells were seeded at about 5×10^6 cells/well into 6-well plates and incubated for 24 h at 37°C under the indicated treatments. Culture medium was collected and subjected to a glucose assay kit (Abcam, ab136955) and a lactate assay kit (Solarbio, BC2335) to measure glucose consumption and lactate production according to the manufacturer's instructions.

2.11 Cell immunofluorescence assay

Cells in the logarithmic growth phase were lifted, centrifuged, and the cell density was adjusted to inoculate into 12-well plates, with three replicate wells in each group. Cells were cultured overnight, fixed in paraformaldehyde for 30 min, washed three times with PBS, and incubated with primary antibodies overnight. The next day, primary antibodies were washed off and secondary antibodies were added and incubated with cells for 2 h. Then, secondary antibodies were washed off and cells were incubated with DAPI staining solution for 15 min. DAPI staining solution was washed off, and cells were photographed under a fluorescence microscope.

2.12 Bioinformatics analyses

The Cancer Genome Atlas (TCGA) and Genotype Tissue Expression (GTEx) databases were queried using the online GEPIA toolset [19]. Analysis of functional interactions among proteins was performed using the STRING online tool [20] and protein-protein interaction network graphs (PPI Network) were generated.

2.13 Statistical Analyses

Data were analyzed using SPSS Version 25.0 (IBM Corp., Armonk, NY, USA), GraphPad Prism 9 software (GraphPad Inc. La Jolla, CA, USA), and Origin Pro 2018C (OriginLab Corp., MA, USA). R Statistical Software version 3.6.3 was used for visualization of survival curves for Kaplan-Meier analysis. Data are presented as the mean ± the standard deviation (SD). The overall survival of patients with PAAD with

high and low RAB10 levels was compared using Kaplan–Meier survival analysis and log-rank tests. A two-tailed Student's t-test was used to compare the statistical differences between two groups. A chi squared test was used to analyze the relationship between RAB10 expression and PAAD clinicopathological features. A p-value of $p < 0.05$ was used to indicate a statistically significant difference.

3. Results

3.1 Overexpression of RAB10 in PAAD samples

We first used the online GEPIA tool set to query the Cancer Genome Atlas (TCGA) and Genotype Tissue Expression (GTEx) databases. We compared differences in RAB10 expression between PAAD samples and normal pancreatic samples. RAB10 expression was significantly increased in PAAD samples (n = 179) compared with normal pancreatic tissue control samples (n = 171) (Fig.1a; $p < 0.001$). To validate these findings in an independent sample cohort, we performed IHC staining on tissue sections to evaluate RAB10 protein expression in tissue samples from 117 PAAD tumors and 32 normal pancreatic tissue samples. Among all PAAD samples, 84 patients (71.8%) had high RAB10 expression and 33 patients (28.2%) had low RAB10 expression. In contrast, among normal pancreatic tissue samples, only 11 patients (34.4%) had high RAB10 expression and 21 patients (65.6%) had low RAB10 expression. Overall, RAB10 expression was significantly increased in pancreatic tumor tissue samples (Fig. 1b; $p < 0.001$).

3.2 High RAB10 expression correlates with clinicopathological features in PAAD patients and predicts poor prognosis.

We next evaluated the association between RAB10 expression levels and clinicopathological features of PAAD patients. RAB10 overexpression was significantly related to T classification and pathological stage, and was unrelated to patient age, sex, clinical stage, N classification, metastasis status, nervous invasion, or venous invasion status (Table 1; $p < 0.05$).

Kaplan-Meier survival analysis and log-rank tests were performed on data from 177 PAAD patients in the TCGA dataset (Fig.1c; $p < 0.01$). The same methods were used to validate the data in a cohort of 86 patients with PAAD, to analyze the relationship between overall survival (OS) and RAB10 expression, and to determine the prognostic value of RAB10 expression in PAAD. Patients with high RAB10 expression had lower OS compared with those with low RAB10 expression (Fig. 1d; $p < 0.01$).

Next, the relationship between risk factors and PAAD prognosis was subjected to univariate and multivariate COX regression analyses (Table 2). RAB10 expression, clinical stage, T, N, M classification, pathological differentiation, and vascular invasion were correlated significantly with prognosis upon univariate Cox regression analysis ($p < 0.05$). Multivariate Cox regression analysis showed that RAB10 expression was an independent prognostic factor ($p = 0.02$). In summary, RAB10 expression may be used as an independent prognostic factor of poor outcomes in PAAD.

Table1

Correlations between RAB10 expression and clinicopathologic features in 86 PAAD patients

Characteristics RAB10	RAB10		
	Low (n=24)	High (n=62)	*P* value (χ2 test)
Age (year)			
≦ 60	10	26	0.982
> 60	14	36	
Gender			
Male	9	31	0.297
Female	15	31	
Clinical stage			
I, II	22	49	0.285
III, IV	2	13	
T classification			
T1, T2	16	26	0.04*
T3, T4	8	36	
N classification			
N0	14	30	0.408
N1, N2	10	32	
Metastasis			
No	24	60	1.000
Yes	0	2	
Pathological differentiation			
1, 2	19	34	0.037*
3, 4	5	28	
Venous invasion			
No	18	43	0.605
Yes	6	19	
Nervous invasion			
No	8	11	0.118
Yes	16	51	

Table 2

Univariate and multivariate Cox regression analyses of prognostic parameters in PAAD patients.

	Univariate analysis		Multivariate analysis	
Characteristics	HR(95% CI)	P value	HR(95% CI)	P value
Age	0.844 (0.536-1.330)	0.465		
Gender	1.072 (0.687-1.673)	0.761		
Clinical stage	1.985 (1.127-3.497)	0.018	0.994 (0.508-1.946)	0.986
T classification	1.594 (1.016-2.502)	0.042	1.414 (0.864-2.314)	0.168
N classification	2.230 (1.415-3.512)	<0.001	1.677 (0.964-2.916)	0.067
Metastasis	17.583 (3.650-84.701)	<0.001	7.361 (1.403-38.629)	0.018*
Pathological differentiation	2.452 (1.533-3.923)	<0.001	1.826 (1.060-3.145)	0.030*
Venous invasion	0.966 (0.584-1.597)	0.891		
Nervous invasion	1.787 (1.027-3.108)	0.040	1.508 (0.847-2.684)	0.162
RAB10 expression	2.521 (1.461-4.351)	<0.001	1.995 (1.114-3.573)	0.020*

3.3 RAB10 knockdown inhibits PAAD cell proliferation, metastatic behavior, and invasion in vitro

We next assessed the expression of RAB10 via qRT-PCR in normal pancreatic cell line (HPDE) and five PAAD cell lines (PANC-1, SW1990, AsPC-1, CFPAC-1, HPAF-II) (Fig. 1e; $p < 0.01$). RAB10 mRNA levels were significantly overexpressed in PAAD cell lines compared with normal pancreatic cell lines. Subsequently, we picked the cell lines with the highest RAB10 mRNA content, the carcinoma *in situ* cell line (PANC-1), and the metastatic cancer cell line CFPAC-1, for subsequent functional testing.

RAB10 knockdown cell lines were constructed from these PAAD cells via transfection of an empty plasmid or the si-RAB10 constructs. Transfection efficiency was confirmed via qRT-PCR and western blot (Fig. 2a, b). These cells were then used for CCK-8, wound healing, and transwell assays. RAB10 knockdown cell lines exhibited reduced tumor cell proliferation, invasion, and migration (Fig. 2c-g).

3.4 RAB10 knockdown inhibits glucose uptake and lactate production in PAAD cells

Uptake of glucose is essential for PAAD cells. Given the role of RAB10 on glucose transporter translocation in adipocytes, we examined the glucose uptake ability and lactate production of cells in PAAD cell lines. The glucose uptake ability and lactate production of RAB10-knockdown PAAD cells were

significantly reduced compared with the control group (Fig.2h, i). We hypothesize that knockdown of RAB10 may inhibit the Warburg effect in PAAD cells *in vitro*.

3.5 GLUT1 is a possible target of RAB10

We further explored the glucose transporters that RAB10 may interfere with in PAAD cells. We queried The Cancer Genome Atlas (TCGA) and the Genotype Tissue Expression (GTEx) databases using the online GEPIA toolset, and we compared the expression differences of Solute carrier family 2 (facilitated glucose transporter, GLUT), members 1~4 in PAAD samples and normal pancreatic samples. GLUT1 and GLUT3 showed differential expression in PAAD samples, and GLUT4 expression was extremely low in PAAD samples (Fig. 3a-d). PPI Network analysis was generated using the online STRING tool, and RAB10 was found to have a direct action relationship only with GLUT1 and GLUT4, and an indirect relationship with GLUT2 and GLUT3 (Fig. 3e).

The mRNA and protein expression of GLUT1 and GLUT3 in the RAB10 knockdown cells was examined using western blot and qRT-PCR. GLUT1 was significantly down-regulated in the si-RAB10 group compared with the control group (Fig. 3f, g). Interestingly, GLUT3 expression was unaffected by RAB10 knockdown. Subsequently, GLUT1 knockdown cell lines were constructed in these PAAD cells by transfection of an si-GLUT1 construct, and RAB10 and GLUT1 were detected by qRT-PCR and western blot. RAB10 expression was not significantly down-regulated in PAAD cells with knockdown of GLUT1.

3.6 Knockdown of RAB10 gene inhibits GLUT1 translocation to cell membrane

To determine whether RAB10 is involved in GLUT1 translocation to the membrane, we stained cells for GLUT1 and GLUT3 and visualized them by fluorescence microscopy to evaluate protein subcellular localization (Fig. 3h). Similar to the previous results, in RAB10-knockdown cells, the expression of GLUT1 was significantly down-regulated, while GLUT3 was not significantly changed. In addition, we observed that GLUT1 localization on the cell membrane surface was reduced in the si-RAB10 group compared with the control group, and subcellular localization changes of GLUT3 were not observed. This shows that RAB10 plays an important role in the translocation of GLUT1 to the membrane.

In addition, to verify that GLUT1 is downstream of RAB10 and is regulated by RAB10, we knocked down GLUT1 in the PANC-1 cell line and the CFPAC-1 cell line. We evaluated the expression of RAB10 using western blot and qRT-PCR, and the expression of RAB10 in pancreatic cancer cell lines did not change significantly after knocking down GLUT1 (Fig. 4a, b). Meanwhile, knockdown of GLUT1 reduced glucose uptake and lactate production in pancreatic cancer cells (Fig. 4c, d).

4. Discussion

Pancreatic ductal cell carcinoma is highly malignant, has a very poor prognosis, is difficult to diagnose early, and is prone to recurrence or metastasis after surgery, even if the patient has the opportunity to

undergo surgical resection [21, 22]. At present, there are challenges in the early diagnosis and treatment of PAAD, and the search for novel treatments for PAAD is ongoing [23, 24].

In a previous analysis of PAAD TCGA and GTEx database data, we found that RAB10 is highly expressed in PAAD compared to normal pancreatic tissue [19]. To validate the findings, we collected resected specimens from patients undergoing pancreatic surgery in our hospital, and grouped the samples according to pathological findings. IHC staining results validated previous database analysis results. When we further analyzed the clinicopathological features and RAB10 expression of PAAD samples, we found that RAB10 expression was associated with pathological differentiation and T classification. In addition, low expression of RAB10 is associated with better prognosis in PAAD, and RAB10 is considered to be an independent prognostic risk factor in PAAD. Together, these findings suggest that RAB10 may promote PAAD and may be related to the aggressiveness of PAAD.

RAB10 has been mostly studied in non-tumor tissues, such as adipose tissue and neural tissue [25–28]. Recently, high RAB10 expression was found be present in a variety of malignancies, and was shown to be associated with tumorigenesis and progression, predicting a poor prognosis. For example, RAB10 promotes the proliferation and migration of gastric cancer cells in mouse models [12], and RAB10 has also been found to promote chemoresistance in breast cancer [13]. Analysis of differentially expressed genes in stem cell carcinoma using microarray analysis revealed that RAB10 promotes the proliferation of tumor cells by inhibiting the AMPK pathway [29]. Our preliminary cell assay results showed that RAB10 promotes the proliferation, metastasis and invasion of PAAD cells in both *in situ* and metastatic cancer cell lines, which was similar to the performance of RAB10 in other tumors.

We also noted that Rab GTPases promote the Warburg effect in osteosarcoma [30]. The Warburg effect is a unique preference for aerobic glycolysis in tumors, and glucose is an essential substrate for this effect [31, 32]. In the Warburg effect, lactate produced by glycolysis can change the intracellular and extracellular pH, and even enhance the viability of malignant tumor cells [33–35]. To investigate whether RAB10 is involved in the regulation of metabolic reprogramming in PAAD cells, we examined glucose uptake and lactate production in different groups of orthotopic PAAD cells, PANC-1, and in pancreatic adenocarcinoma liver metastasis cells, CFPAC-1. Glucose uptake and lactate production were down-regulated in the si-RAB10 group in both cell lines. This shows that RAB10 is likely to be involved in glucose uptake in PAAD cells.

Rab GTPases are highly conserved vesicular trafficking modulators with the main task of ensuring that cargo is transported to the correct destination, and 66 members of this family have been described in the human genome [36, 37]. The conversion between the GDP- and GTP-bound forms of RAB GTPases is catalyzed by guanine nucleotide exchange factors (GEFs), while Rab molecules are activated by interaction with the TCB domain of GTPase activating proteins (GAPs) [38–40]. These mechanisms have been largely studied, but GAPs have limited specificity [41]. Therefore, it is likely not worthwhile to search for and validate RAB10-related GEFs and GAPs in PAAD. In cancer cells, vesicle trafficking is closely

related to tumor phenotypes such as metabolism, invasion, autophagy, and chemoresistance [42]. Currently, the effects of RAB GTPsaes on cancer cell metabolism has been studied, but the specific details remain unclear. Initially, RAB25 was able to increase ATP and glycogen storage in tumor cells [43]. In the last decade, RAB GTPases were confirmed to be involved in gastric cancer cells by regulating GLUT1 translocate to the cell membrane to regulate glucose uptake [44]. However, it remained unknown whether Rab GTPases are involved in the regulation of other members of the GLUT family. In this study, we initially established a RAB10 knockdown model, and we identified the glucose uptake ability and lactate production ability of PAAD cells with RAB10 knockdown, confirming that RAB10 regulates aspects of metabolism. Afterwards, we analyzed the links between common GLUT family members and RAB10. We found that GLUT1 was the most likely RAB10-regulated GLUT family member.

In conclusion, our results suggest that overexpression of RAB10 in PAAD is associated with worse patient survival outcomes. Down-regulation of RAB10 may inhibit the survival and progression of tumor cells by inhibiting GLUT1 translocate to the cell membrane and by down-regulating GLUT1 expression, which decrease glucose uptake in tumor cells. These data suggest that RAB10 may be a viable prognostic biomarker for assessing patients with PAAD, and may be a viable target for future therapeutic development.

Declarations

Acknowledgements

This work was supported by a grant from the National Natural Science Foundation of China (No. 81772516).

Conflict of interest

The authors have no relevant financial or non-financial interests to disclose.

Ethics approval and consent to participate

The Ethics Committee of Northern Jiangsu People's Hospital approved the study, and all patients provided written informed consent.

Author Contributions

All authors contributed to the study conception and design. Material preparation were performed by Lijie Cai, Tongtai Liu and Jie Yao. Data collection and analysis were performed by Lijie Cai, Jinrui Han, Junqing Wu, Xinyu Ge, Peng Liu and Heng Duan. The first draft of the manuscript was written by Lijie Cai and all authors commented on previous versions of the manuscript. All authors read and approved the final manuscript.

Authors' information

Lijie Cai, Dalian Medical University, Dalian 116044, Liaoning, People's Republic of China, E-mail: doccai@outlook.com, OCRID: 0000-0001-8149-0547

Jinrui Han, Dalian Medical University, Dalian 116044, Liaoning, People's Republic of China, E-mail: hanjr1996@163.com

Junqing Wu, Medical College of Yangzhou University, Yangzhou, Jiangsu 225001, People's Republic of China, E-mail: 727280445@qq.com

Xinyu Ge, Dalian Medical University, Dalian 116044, Liaoning, People's Republic of China, email: 491604351@qq.com

Peng Liu, Medical College of Yangzhou University, Yangzhou, Jiangsu 225001, People's Republic of China, E-mail: 2233400780@qq.com

Heng Duan, Dalian Medical University, Dalian 116044, Liaoning, People's Republic of China, E-mail: 528737769@qq.com

Tongtai Liu, Department of Hepatobiliary and Pancreatic Surgery, Northern Jiangsu People's Hospital, Nantong Western Road, Guangling Qu, Yangzhou, Jiangsu 225001, People's Republic of China, E-mail: liutongtai@tom.com

Jie, Yao, Department of Hepatobiliary and Pancreatic Surgery, Northern Jiangsu People's Hospital, Nantong Western Road, Guangling Qu, Yangzhou, Jiangsu 225001, People's Republic of China, E-mail: dryaojie@yzu.edu.cn, OCRID:0000-0001-5447-893X

References

1. Siegel RL, Miller KD, Jemal A. (2020) Cancer statistics, 2020. CA Cancer J Clin. 70:https://doi.org/10.3322/caac.21590
2. Hidalgo M, Cascinu S, Kleeff J, Labianca R, Löhr JM, et al. (2015) Addressing the challenges of pancreatic cancer: future directions for improving outcomes. Pancreatology. 15:https://doi.org/10.1016/j.pan.2014.10.001
3. Halbrook CJ, Lyssiotis CA. (2017) Employing Metabolism to Improve the Diagnosis and Treatment of Pancreatic Cancer. Cancer Cell. 31:https://doi.org/10.1016/j.ccell.2016.12.006
4. Vander Heiden MG, Cantley LC, Thompson CB. (2009) Understanding the Warburg effect: the metabolic requirements of cell proliferation. Science. 324:1029-33. https://doi.org/10.1126/science.1160809
5. de la Cruz-López KG, Castro-Muñoz LJ, Reyes-Hernández DO, García-Carrancá A, Manzo-Merino J. (2019) Lactate in the Regulation of Tumor Microenvironment and Therapeutic Approaches. Front Oncol. 9:1143. https://doi.org/10.3389/fonc.2019.01143

6. English AR, Voeltz GK. (2013) Rab10 GTPase regulates ER dynamics and morphology. Nat Cell Biol. 15:169-78. https://doi.org/10.1038/ncb2647
7. Jaldin-Fincati JR, Pavarotti M, Frendo-Cumbo S, Bilan PJ, Klip A. (2017) Update on GLUT4 Vesicle Traffic: A Cornerstone of Insulin Action. Trends Endocrinol Metab. 28:597-611. https://doi.org/10.1016/j.tem.2017.05.002
8. Brumfield A, Chaudhary N, Molle D, Wen J, Graumann J, McGraw TE. (2021) Insulin-promoted mobilization of GLUT4 from a perinuclear storage site requires RAB10. Mol Biol Cell. 32:57-73. https://doi.org/10.1091/mbc.E20-06-0356
9. Sano H, Peck GR, Kettenbach AN, Gerber SA, Lienhard GE. (2011) Insulin-stimulated GLUT4 protein translocation in adipocytes requires the Rab10 guanine nucleotide exchange factor Dennd4C. J Biol Chem. 286:16541-5. https://doi.org/10.1074/jbc.C111.228908
10. Bruno J, Brumfield A, Chaudhary N, Iaea D, McGraw TE. (2016) SEC16A is a RAB10 effector required for insulin-stimulated GLUT4 trafficking in adipocytes. J Cell Biol. 214:61-76. https://doi.org/10.1083/jcb.201509052
11. Wen Z, Xiong D, Zhang S, Liu J, Li B, et al. (2021) Case Report: : A Novel Fusion in a Patient With Gastric Cancer. Front Oncol. 11:645370. https://doi.org/10.3389/fonc.2021.645370
12. Wei F, Wang Y, Zhou Y, Li Y. (2021) Long noncoding RNA CYTOR triggers gastric cancer progression by targeting miR-103/RAB10. Acta Biochim Biophys Sin (Shanghai). 53:1044-54. https://doi.org/10.1093/abbs/gmab071
13. Li Y, Xiong Y, Wang Z, Han J, Shi S, et al. (2021) FAM49B promotes breast cancer proliferation, metastasis, and chemoresistance by stabilizing ELAVL1 protein and regulating downstream Rab10/TLR4 pathway. Cancer Cell Int. 21:534. https://doi.org/10.1186/s12935-021-02244-9
14. Shen G, Mao Y, Su Z, Du J, Yu Y, Xu F. (2020) PSMB8-AS1 activated by ELK1 promotes cell proliferation in glioma via regulating miR-574-5p/RAB10. Biomed Pharmacother. 122:109658. https://doi.org/10.1016/j.biopha.2019.109658
15. Seguin L, Odouard S, Corlazzoli F, Haddad SA, Moindrot L, et al. (2021) Macropinocytosis requires Gal-3 in a subset of patient-derived glioblastoma stem cells. Commun Biol. 4:718. https://doi.org/10.1038/s42003-021-02258-z
16. Dai S, Li N, Zhou M, Yuan Y, Yue D, et al. (2021) LncRNA EBLN3P promotes the progression of osteosarcoma through modifying the miR-224-5p/Rab10 signaling axis. Sci Rep. 11:1992. https://doi.org/10.1038/s41598-021-81641-6
17. Chun YS, Pawlik TM, Vauthey J-N. (2018) 8th Edition of the AJCC Cancer Staging Manual: Pancreas and Hepatobiliary Cancers. Ann Surg Oncol. 25:845-7. https://doi.org/10.1245/s10434-017-6025-x
18. Bustin SA, Benes V, Garson JA, Hellemans J, Huggett J, et al. (2009) The MIQE guidelines: minimum information for publication of quantitative real-time PCR experiments. Clin Chem. 55:611-22. https://doi.org/10.1373/clinchem.2008.112797
19. Tang Z, Li C, Kang B, Gao G, Li C, Zhang Z. (2017) GEPIA: a web server for cancer and normal gene expression profiling and interactive analyses. Nucleic Acids Res.

45:https://doi.org/10.1093/nar/gkx247

20. Szklarczyk D, Gable AL, Nastou KC, Lyon D, Kirsch R, et al. (2021) The STRING database in 2021: customizable protein-protein networks, and functional characterization of user-uploaded gene/measurement sets. Nucleic Acids Res. 49:D605-D12. https://doi.org/10.1093/nar/gkaa1074
21. Park W, Chawla A, O'Reilly EM. (2021) Pancreatic Cancer: A Review. JAMA. 326:851-62. https://doi.org/10.1001/jama.2021.13027
22. Ettrich TJ, Seufferlein T. (2021) Systemic Therapy for Metastatic Pancreatic Cancer. Curr Treat Options Oncol. 22:106. https://doi.org/10.1007/s11864-021-00895-4
23. O'Neill RS, Stoita A. (2021) Biomarkers in the diagnosis of pancreatic cancer: Are we closer to finding the golden ticket? World J Gastroenterol. 27:4045-87. https://doi.org/10.3748/wjg.v27.i26.4045
24. Yang J, Xu R, Wang C, Qiu J, Ren B, You L. (2021) Early screening and diagnosis strategies of pancreatic cancer: a comprehensive review. Cancer Commun (Lond). 41:1257-74. https://doi.org/10.1002/cac2.12204
25. Wauters F, Cornelissen T, Imberechts D, Martin S, Koentjoro B, et al. (2020) mutations impair depolarization-induced mitophagy through inhibition of mitochondrial accumulation of RAB10. Autophagy. 16:203-22. https://doi.org/10.1080/15548627.2019.1603548
26. Atashrazm F, Hammond D, Perera G, Bolliger MF, Matar E, et al. (2019) LRRK2-mediated Rab10 phosphorylation in immune cells from Parkinson's disease patients. Mov Disord. 34:406-15. https://doi.org/10.1002/mds.27601
27. Liu Y, Xu X-H, Chen Q, Wang T, Deng C-Y, et al. (2013) Myosin Vb controls biogenesis of post-Golgi Rab10 carriers during axon development. Nat Commun. 4:2005. https://doi.org/10.1038/ncomms3005
28. Sano H, Eguez L, Teruel MN, Fukuda M, Chuang TD, et al. (2007) Rab10, a target of the AS160 Rab GAP, is required for insulin-stimulated translocation of GLUT4 to the adipocyte plasma membrane. Cell Metab. 5:293-303.
29. Zhang Y-J, Pan Q, Yu Y, Zhong X-P. (2020) microRNA-519d Induces Autophagy and Apoptosis of Human Hepatocellular Carcinoma Cells Through Activation of the AMPK Signaling Pathway via Rab10. Cancer Manag Res. 12:2589-602. https://doi.org/10.2147/CMAR.S207548
30. Cheng JC, McBrayer SK, Coarfa C, Dalva-Aydemir S, Gunaratne PH, et al. (2013) Expression and phosphorylation of the AS160_v2 splice variant supports GLUT4 activation and the Warburg effect in multiple myeloma. Cancer Metab. 1:14. https://doi.org/10.1186/2049-3002-1-14
31. Hirschey MD, DeBerardinis RJ, Diehl AME, Drew JE, Frezza C, et al. (2015) Dysregulated metabolism contributes to oncogenesis. Semin Cancer Biol. 35 Suppl:S129-S50. https://doi.org/10.1016/j.semcancer.2015.10.002
32. Cao L, Wu J, Qu X, Sheng J, Cui M, et al. (2020) Glycometabolic rearrangements--aerobic glycolysis in pancreatic cancer: causes, characteristics and clinical applications. J Exp Clin Cancer Res. 39:267. https://doi.org/10.1186/s13046-020-01765-x

33. Kamisawa T, Wood LD, Itoi T, Takaori K. (2016) Pancreatic cancer. Lancet. 388:73-85. https://doi.org/10.1016/S0140-6736(16)00141-0
34. Gatenby RA, Gillies RJ. (2004) Why do cancers have high aerobic glycolysis? Nat Rev Cancer. 4:891-9.
35. Sun S, Li H, Chen J, Qian Q. (2017) Lactic Acid: No Longer an Inert and End-Product of Glycolysis. Physiology (Bethesda). 32:453-63. https://doi.org/10.1152/physiol.00016.2017
36. Li G, Marlin MC. (2015) Rab family of GTPases. Methods Mol Biol. 1298:https://doi.org/10.1007/978-1-4939-2569-8_1
37. Homma Y, Hiragi S, Fukuda M. (2021) Rab family of small GTPases: an updated view on their regulation and functions. FEBS J. 288:36-55. https://doi.org/10.1111/febs.15453
38. Stenmark H. (2009) Rab GTPases as coordinators of vesicle traffic. Nat Rev Mol Cell Biol. 10:513-25. https://doi.org/10.1038/nrm2728
39. Delprato A, Merithew E, Lambright DG. (2004) Structure, exchange determinants, and family-wide rab specificity of the tandem helical bundle and Vps9 domains of Rabex-5. Cell. 118:607-17.
40. Eathiraj S, Pan X, Ritacco C, Lambright DG. (2005) Structural basis of family-wide Rab GTPase recognition by rabenosyn-5. Nature. 436:415-9.
41. Haas AK, Yoshimura S-i, Stephens DJ, Preisinger C, Fuchs E, Barr FA. (2007) Analysis of GTPase-activating proteins: Rab1 and Rab43 are key Rabs required to maintain a functional Golgi complex in human cells. J Cell Sci. 120:2997-3010.
42. Jin H, Tang Y, Yang L, Peng X, Li B, et al. (2021) Rab GTPases: Central Coordinators of Membrane Trafficking in Cancer. Front Cell Dev Biol. 9:648384. https://doi.org/10.3389/fcell.2021.648384
43. Cheng KW, Agarwal R, Mitra S, Lee J-S, Carey M, et al. (2012) Rab25 increases cellular ATP and glycogen stores protecting cancer cells from bioenergetic stress. EMBO Mol Med. 4:125-41. https://doi.org/10.1002/emmm.201100193
44. Yang R, Liu G, Han L, Qiu Y, Wang L, Wang M. (2021) MiR-365a-3p-Mediated Regulation of HELLS/GLUT1 Axis Suppresses Aerobic Glycolysis and Gastric Cancer Growth. Front Oncol. 11:616390. https://doi.org/10.3389/fonc.2021.616390

Figures

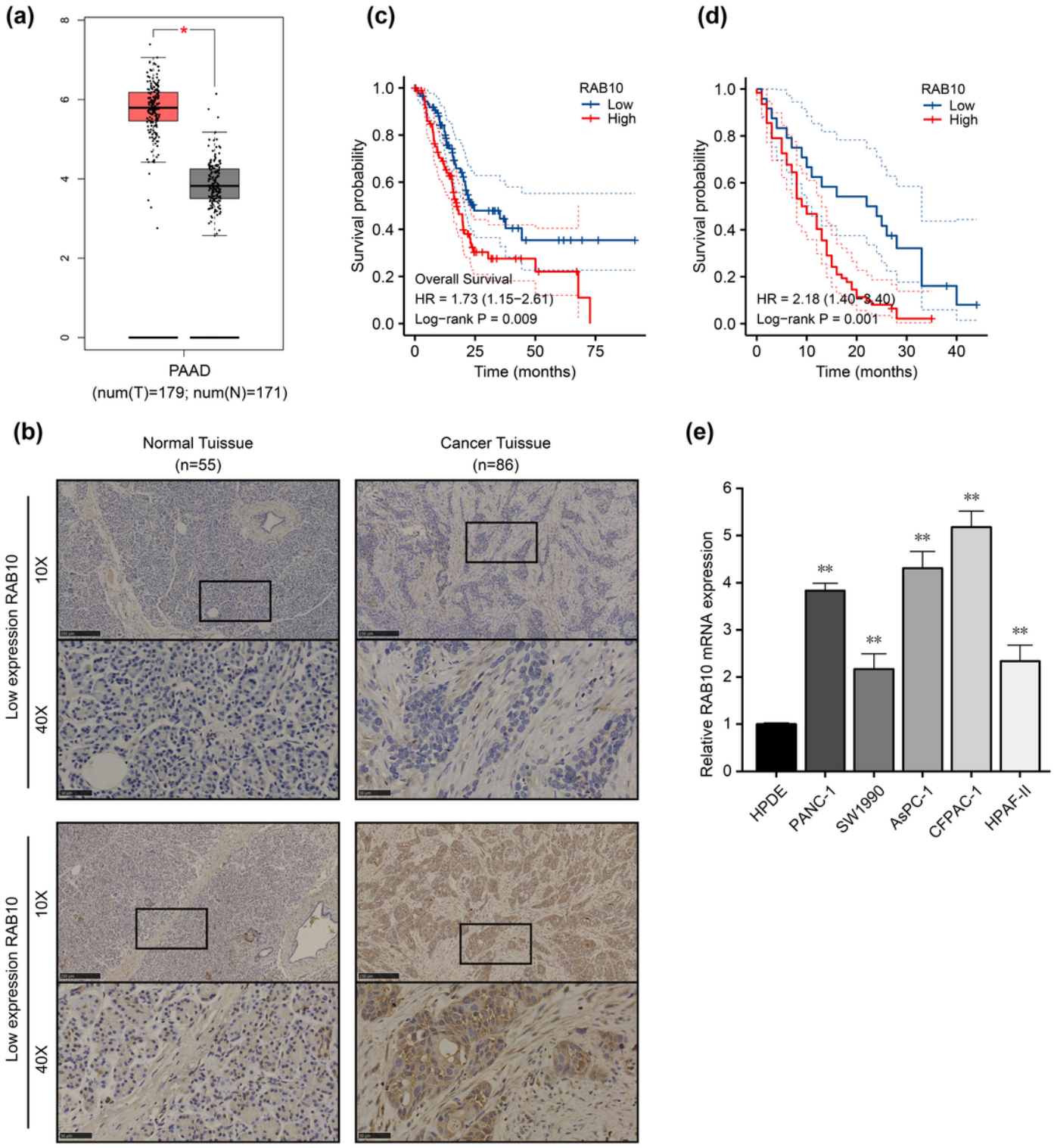

Figure 1

RAB10 expression is elevated in PAAD. **a** TCGA and GTEx databases show high expression of RAB10 in human pancreatic cancer tissues. The red box represents PAAD tumor tissue and the gray box represents normal pancreatic tissue. **b** Representative images of both RAB10 negative and RAB10 positive samples with 10x objective and 40x objective, respectively. **c** Kaplan-Meier curves generated using clinical data of PAAD patients from the TCGA database showed that high RAB10 predicted poor prognosis ($p < 0.01$). **d**

Clinical information collected from 86 PAAD patients in this study generated Kaplan-Meier curves demonstrating a significant relationship between high RAB10 expression and poor overall survival ($p < 0.01$). **e** Expression levels of RAB10 in pancreatic cancer cell lines determined by qRT-PCR. RAB10: RAB10, member of the RAS oncogene family; TCGA: The Cancer Genome Atlas; GTEx: Genotype-Tissue Expression; qRT-PCR: real-time quantitative polymerase chain reaction

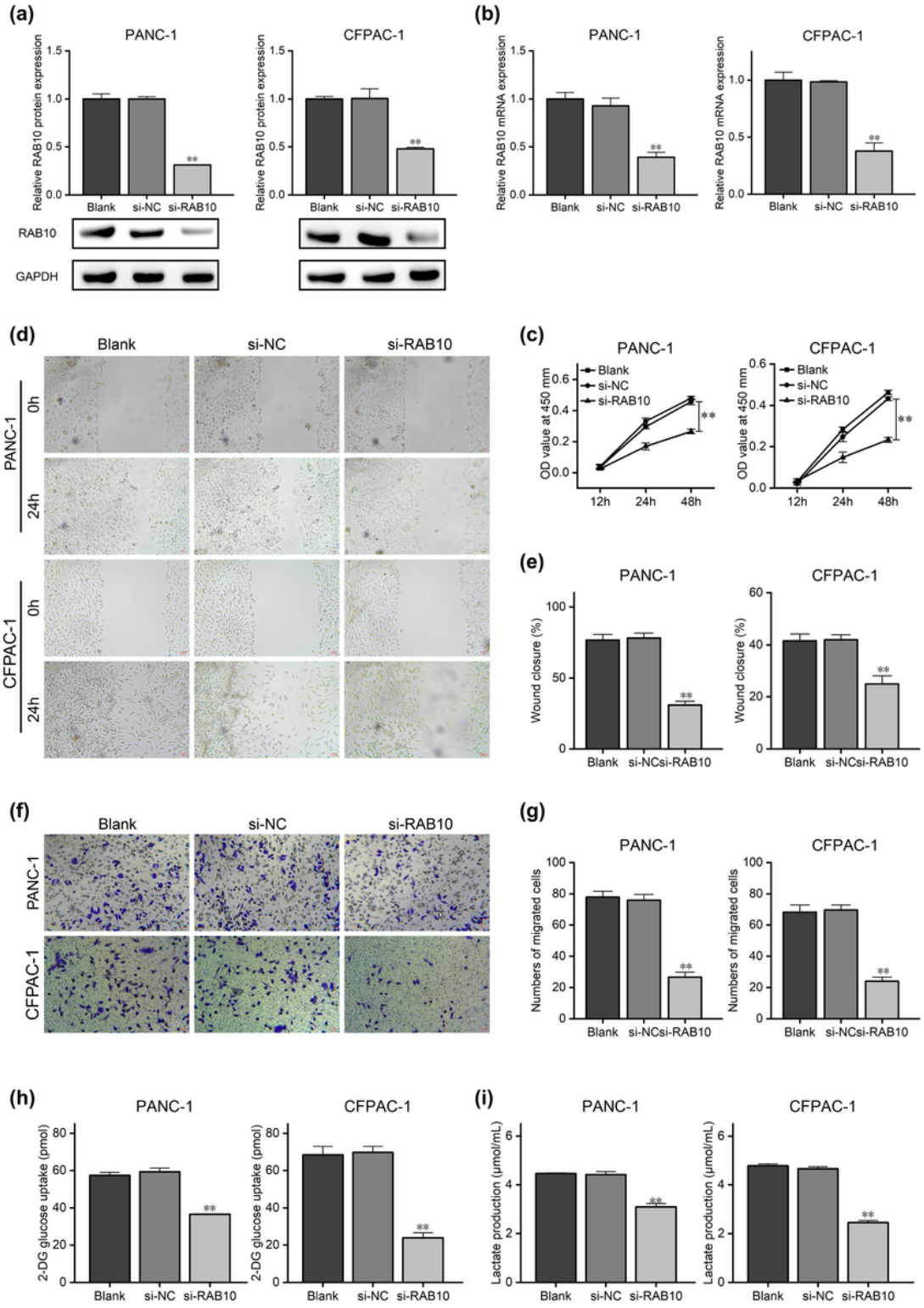

Figure 2

Knockdown of RAB10 inhibits the malignant characteristics of PAAD cells. **a, b** Western blot (a) and qRT-PCR (b) were used to quantify the efficiency of RAB10 knockdown in pancreatic cancer cell lines. **c** The effects of RAB10 knockdown on PAAD cell proliferation was assessed by CCK-8 analysis. **d, e** Wound healing assays were used to assess the effects of RAB10 knockdown on PAAD cell migration. **f, g** Transwell migration assays was used to assess the effects of RAB10 knockdown on PAAD cell invasion. **h** Glucose uptake assays were used to assess the effects of RAB10 knockdown on glucose uptake capacity. **i** Lactate production assay experiments were used to assess the effect of RAB10 knockdown on the amount of lactic acid produced. Data are shown as mean ± SD (*$p < 0.05$, ** $p < 0.01$, *** $p < 0.001$) from triplicate samples in three independent experiments. CCK-8: Cell Counting Kit-8; RT-qPCR: real-time quantitative polymerase chain reaction; SD: standard deviation.

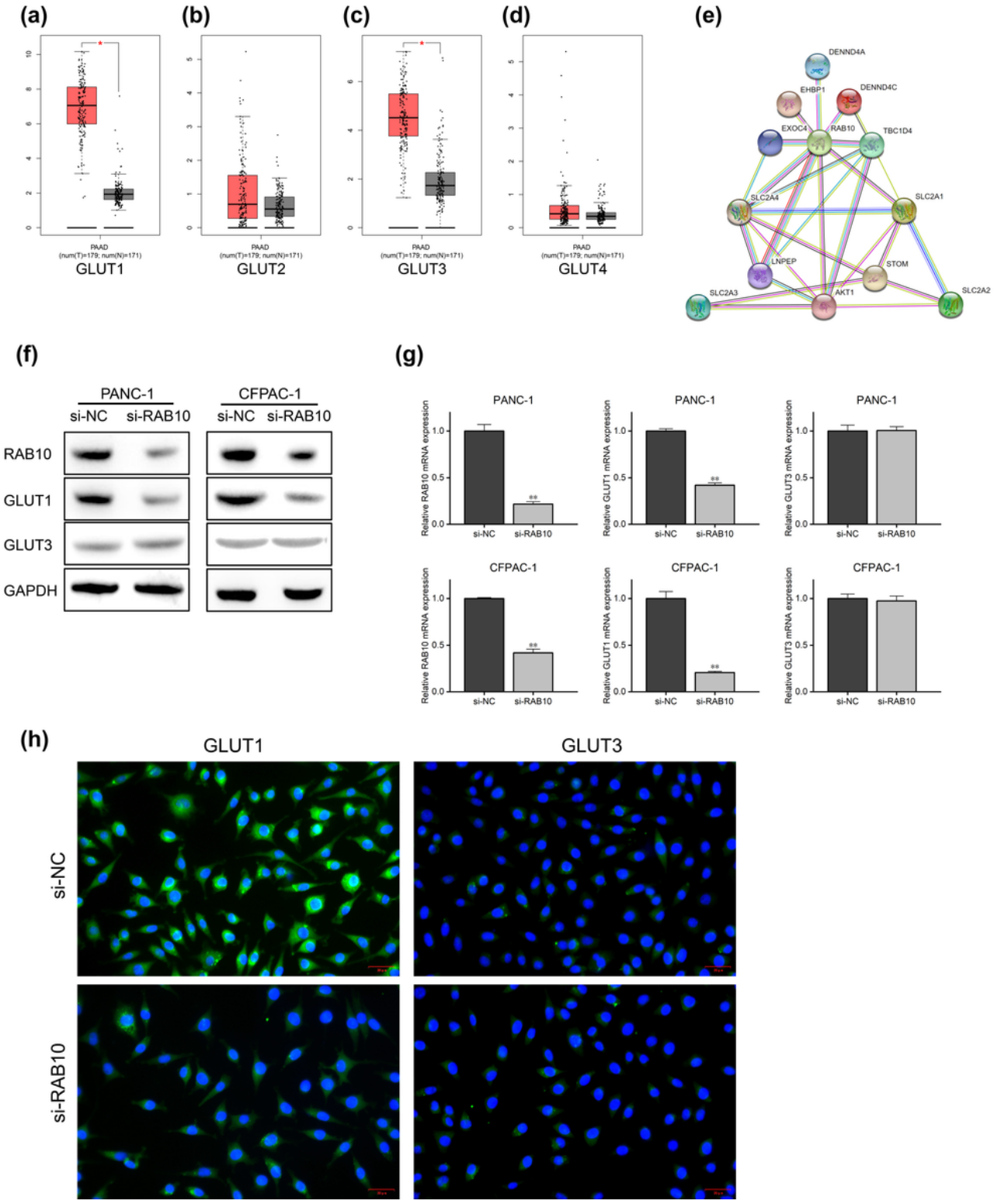

Figure 3

a-d TCGA and GTEx databases show differential expression of common GLUT members in human PAAD tissue. GLUT1 (a), GLUT2 (b), GLUT3 (c), GLUT4 (d) from left to right, respectively. **e** PPI network graph generated using the STRING online tool, where GLUT1-4 are shown as SLC2A1-4 in Figure. **f, g** Western blot (f) and qRT-PCR (g) were used to examine the effects of RAB10 knockdown on mRNA transcription and protein expression of GLUT1 and GLUT3 in pancreatic cancer cells. **h** Cell immunofluorescence

assays showed that knockdown of RAB10 allowed GLUT1 to accumulate less on the membrane surface and GLUT3 to be barely affected. Nuclei were stained using DAPI (blue) and GLUT1 and GLUT3 are indicated by green fluorescence. GLUT1: Glucose transporter 1, facilitated solute carrier family 2 member 1, SLC2A1. The same naming conventions apply to GLUT1, GLUT2, GLUT3, and GLUT4.

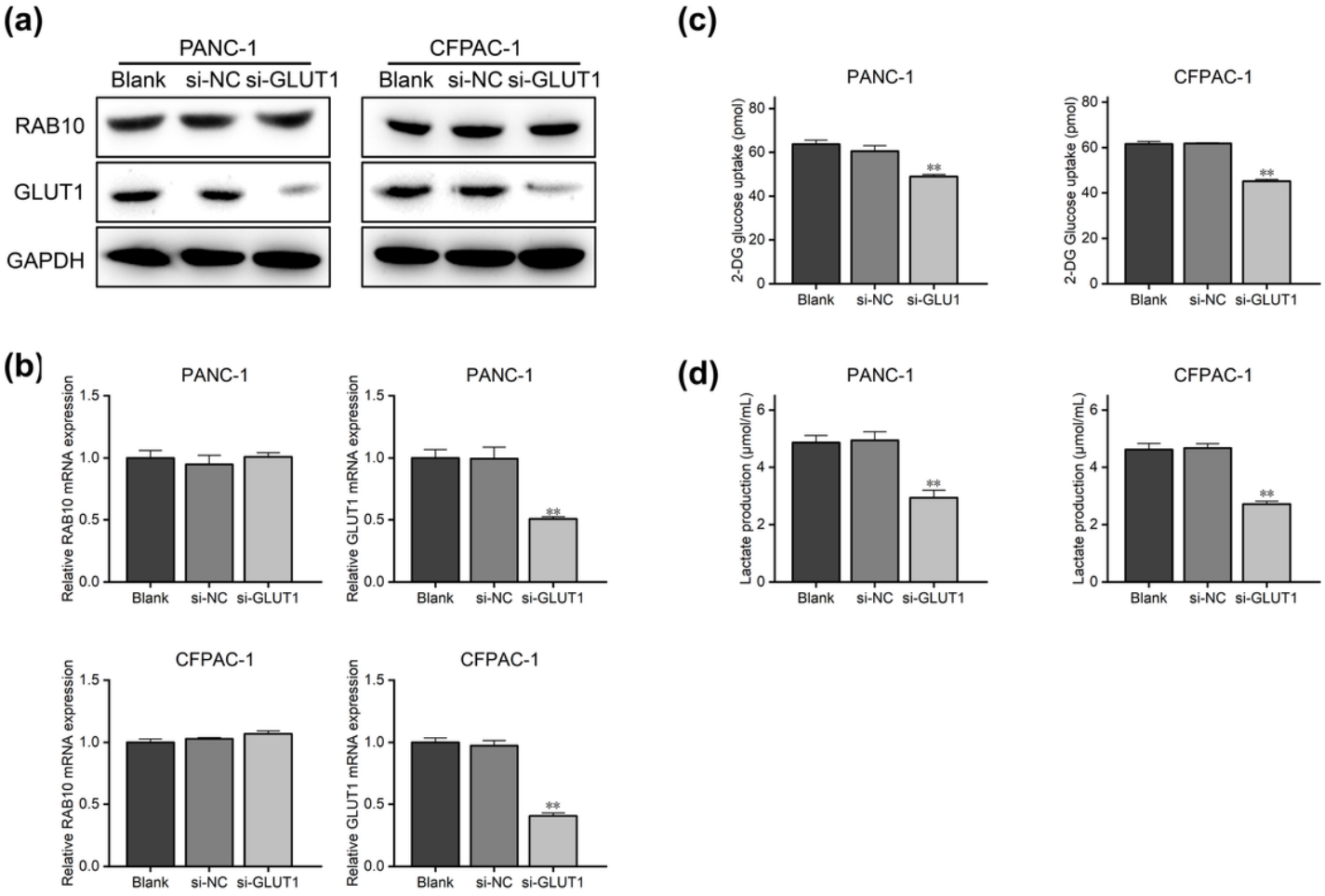

Figure 4

a, b Western blot (a) and qRT-PCR (b) were used to determine the knockdown efficiency of GLUT1 and RAB10 expression in pancreatic cancer cell lines. **c** The glucose uptake assay was used to assess the effects of GLUT1 knockdown on glucose uptake capacity. **d** Lactate production assays were used to assess the effects of GLUT1 knockdown on lactate production

Supplementary Files

This is a list of supplementary files associated with this preprint. Click to download.

- SupplementaryTable1.xlsx
- SupplementaryTable2.xlsx